

가

가

:

2002 2

2002 12 26

( )

( )

( )

	.....	
<b>1.</b>	.....	<b>1</b>
<b>2.</b>	.....	<b>4</b>
2.1 CFRP	.....	4
2.2 -	.....	6
2.3	.....	8
2.4	.....	11
2.4.1	.....	11
2.4.2	.....	12
<b>3.</b>	.....	<b>15</b>
3.1	.....	15
3.2	.....	21
<b>4.</b>	.....	<b>27</b>
4.1	.....	27
4.2 AE	.....	31
4.3	.....	37
4.4 CCD	.....	41
4.5 SEM	.....	49
<b>5.</b>	.....	<b>55</b>
	.....	<b>57</b>
<b>Abstract</b>	.....	<b>59</b>

$E$  : Modulus of elasticity  
 $\sigma_u$  : Ultimate tensile strength  
 $\epsilon_u$  : Fracture strain rate  
 $\nu$  : Poisson's ratio  
 $R$  : Stress ratio  
 $N_f$  : Fracture cycle in fatigue  
 $S$  : Stress  
 $a$  : Damage length  
 $d$  : Hole diameter

# 1.

,  
가

가 ,  
가 . ,  
(Carbon Fiber Reinforced Plastic, CFRP )

가 . CFRP  
,  
(matrix cracking), ,  
(debonding), (delamination),  
. CFRP 가

가 ,  
가

(1).

(2,3) . CFRP

가

1964 Boller<sup>(4)</sup>

, Owen

(5)

가

, Lawcock<sup>(6)</sup>

가

가

(Acoustic Emission, AE)

1970

(7)

AE

Ni<sup>(8-10)</sup> AE

Chow<sup>(11)</sup> 가 GFRP

AE X

가

CFRP

CFRP 가

가 [0/90]s [90/0]s [0/±45/90]s CFRP

. AE

AE

AE

가

CCD

가 .

(SEM)

[0/90]s, [90/0]s CFRP

CCD

가 .

CFRP

가 .

## 2.

### 2.1 CFRP

가

가 .

(fatigue) .

가

가 가 .

가

가

(stress concentration)

가 (crack

density)가 가 ,

가 .

90°

(12),

## 2.2 -

가

가

가

가

S-N 가

가 (1) <sup>(13)</sup>

$$= UTS - b \log N_f + d \quad (1)$$

가, UTS (Ultimate tensile strength),  $N_f$ , b d

가

가

S-N (fatigue limit) . S-N

1 1

가 S-N

가  $10^6$   $10^7$

가  $10^6$  가

S-N

,

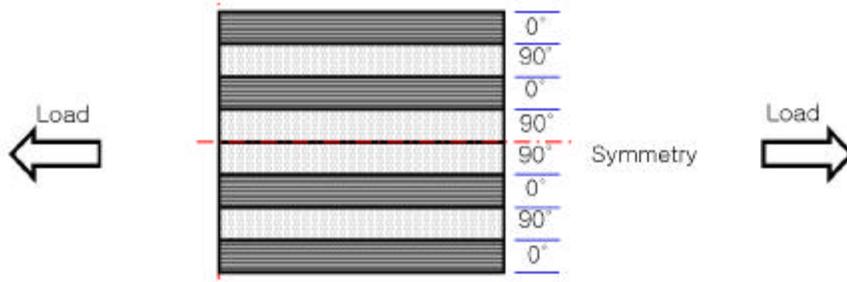
2.3

가  
 . 가  
 가 가  
 . 가  
 . 가  
 . 가 ,  
 . 가  
 가 가 가 가 ,  
 가 0 가 ,  
 가 가 ,  
 가 (ply)  
 가

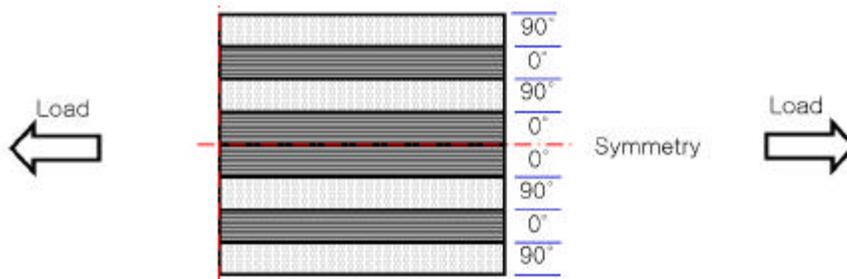
,  
가  
4가 .

가 . ,  
가 ,  
가

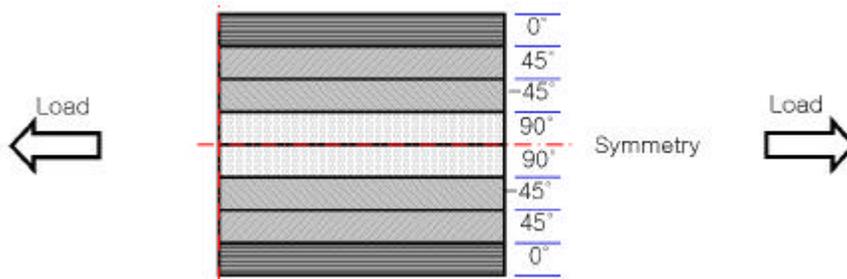
. Fig. 1



(a)  $[0/90]_s$  CFRP



(b)  $[90/0]_s$  CFRP



(c)  $[0/\pm 45/90]_s$  CFRP

**Fig. 1** Lay-up orientation of CFRP laminate composite.

## 2.4

### 2.4.1

가 , 가  
(strain energy) , 가  
가 . 가  
(AE)  
AE  
가 가  
가  
(Non-Destructive Test, NDT)가  
,  
AE 가  
,  
가  
AE  
AE , AE  
(SNR)

가

가

가 .

가

AE

가

, AE가

가

. ,

AE

(event count)

,

.

### 2.4.2

AE

가

가

Hz

20kHz

AE

. AE

<sup>(14)</sup>. AE

,

,

AE

.

AE

가

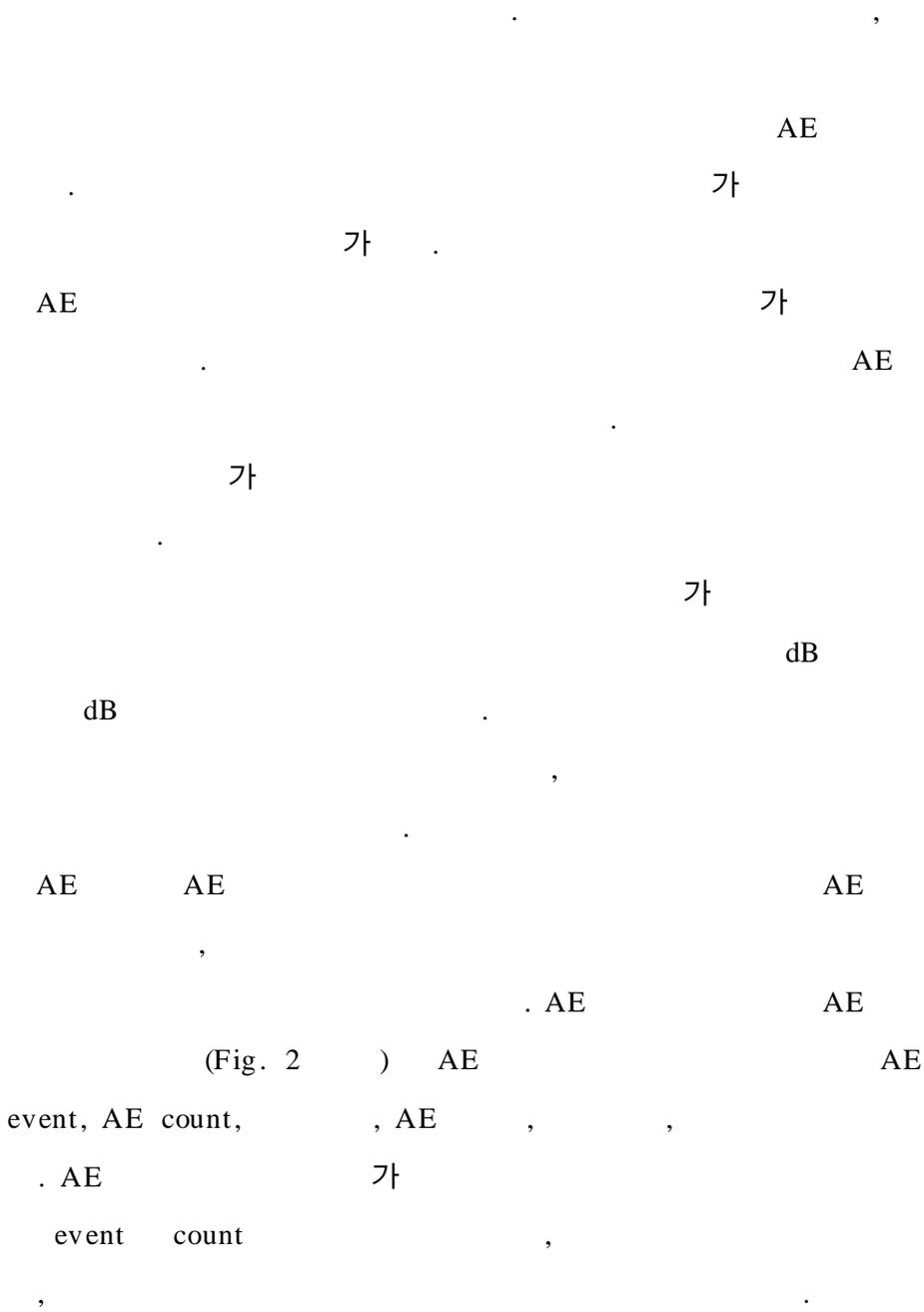


(Fig. 2 ) AE

event, AE count, , AE , ,  
 . AE 가  
 event count ,

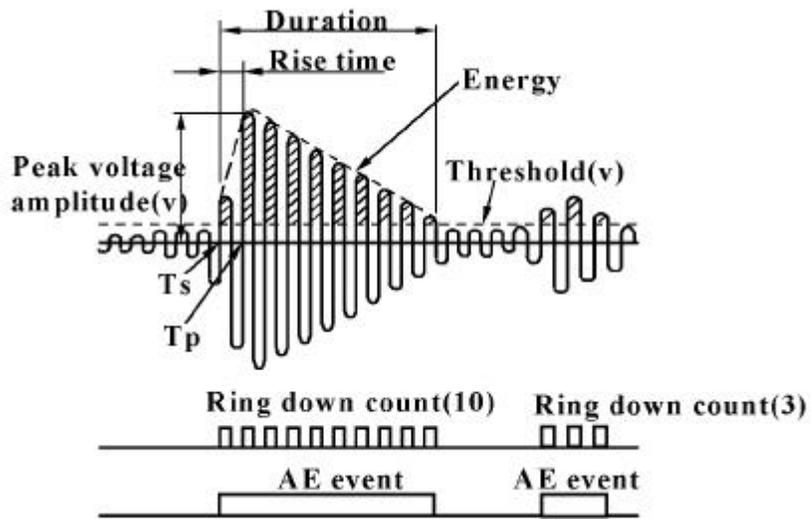


Fig. 2 Parameter of acoustic emission signal analysis.

### 3.

#### 3.1

( ) ,

Low HCU 1003 Table 1

**Table 1** Physical properties of prepreg Low R/C HCU 1003 material

Meterial	CF Wt(gr/m <sup>2</sup> )	Resin Wt(gr/m <sup>2</sup> )	R/C	Scrim Wt(gr/m <sup>2</sup> )	Total Wt(gr/m <sup>2</sup> )	t (mm)
HCU 1003	112	41	27 ± 2	34	155	0.126

(Carbon Fiber Reinforced Prepreg)

가 . 가 , 245mm(Fig. 3 ) [0/90]s [90/0]s [0/ ± 45/90]s 8 (Silicon Oil KS 707) (Hot Press, Fig. 4 ) 150 , 80kg/cm<sup>2</sup> 1 . 1 1 0.9mm가 .

CFRP

(Fig. 5 )

ASTM D-3039-00<sup>(15)</sup>

200mm × 25mm

가

,

가

5mm

가

가

(araldite)

1 : 1

( : 2.0mm)

. #60

-

가

, #220

-

,

가

30°

.

130

30

. Fig. 6

.

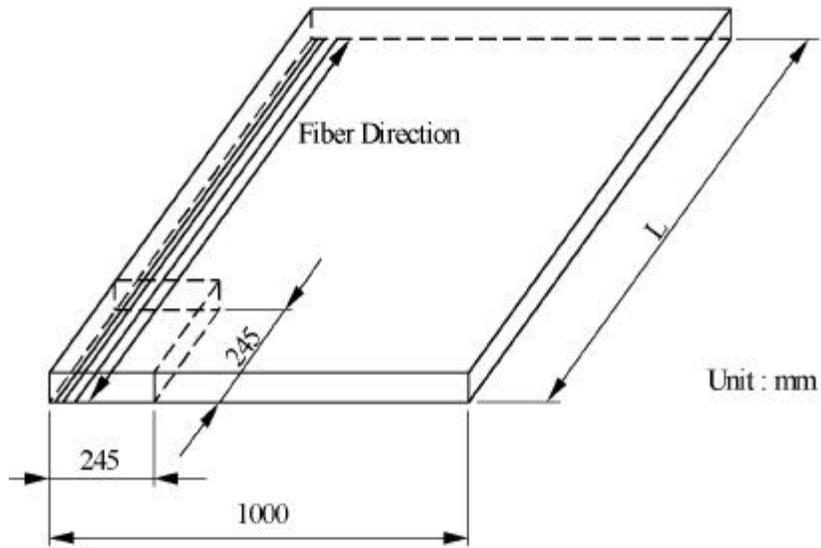


**Fig. 3** Sampling position for CFRP specimen.



**Fig. 4** Hot press.

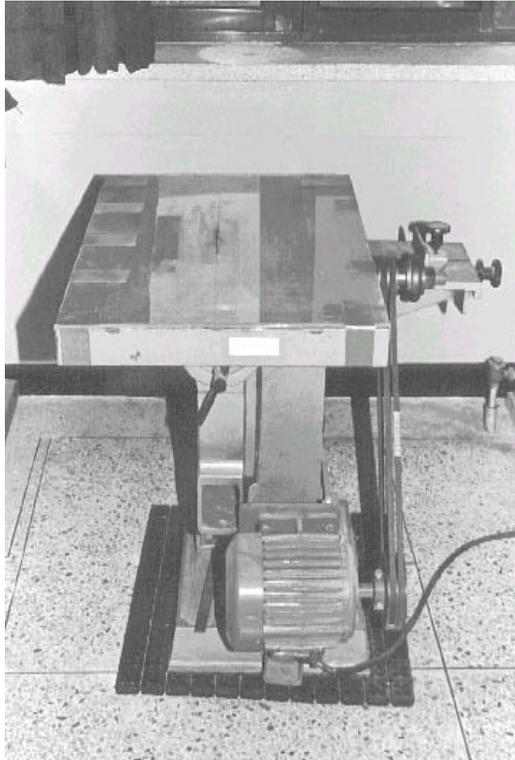


**Fig. 5** Diamond wheel cutter.

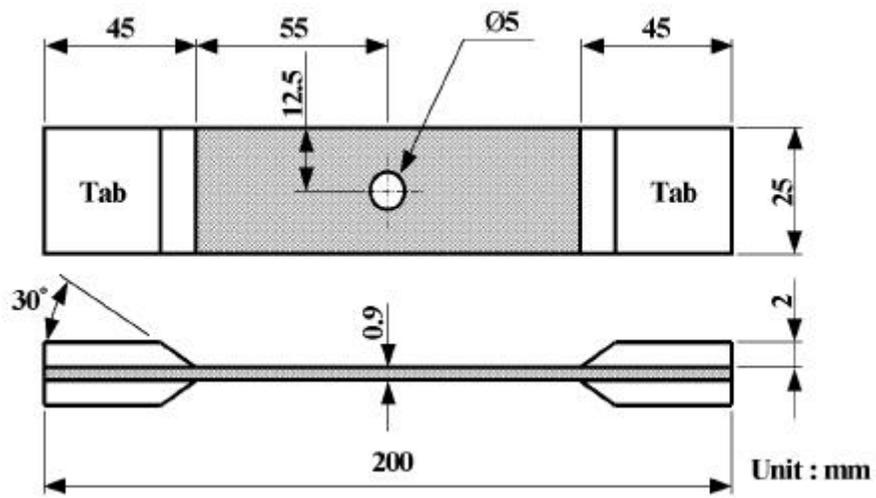
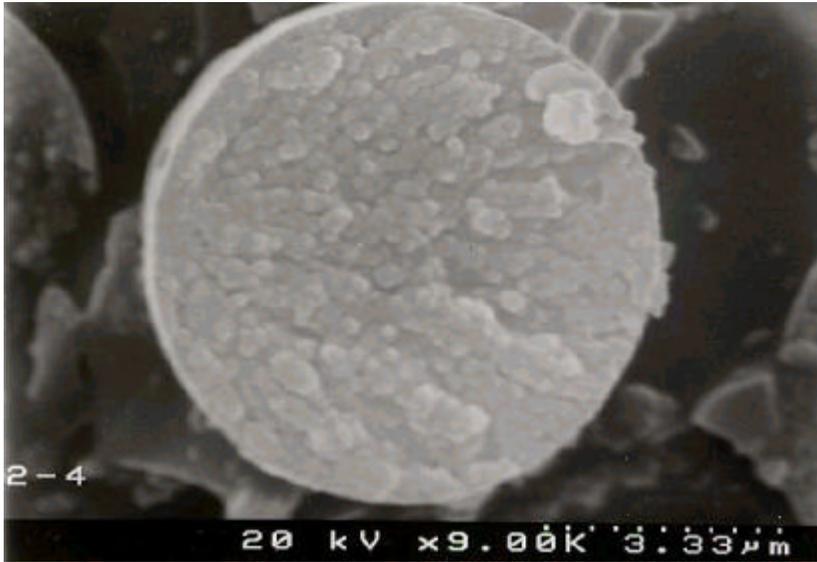


Fig. 6 CFRP specimen configuration.

### 3.2

,  
(H , 5ton)  
ASTM D3039-00<sup>(15)</sup> 0.5mm/min  
(H , 5ton)  
(half sine) -  
0.1  
5Hz S-N  
1 × 10<sup>6</sup>  
DA  
PC 30° 60W S  
TR-850 CCD  
가 PC  
가 0.1 0.2mm  
30  
SEM  
SEM  
SEM  
7.4μm (Fig. 7 ).  
AE PAC AEDSP 32/16 PC  
AE 가 150kHz R15  
( )

, 100kHz 300kHz  
 . Threshold Fixed Threshold 40dB  
 . AEDSP 32/16 , R15 1  
 channel Fig. 8 . AE  
 , AEDSP 32/16 가  
 AE MISTRAS-2  
 001 AE 가 .  
 CCD  
 AE  
 AE 가 . Fig. 9  
 Fig. 10 .



**Fig. 7** SEM photograph of fiber diameter.

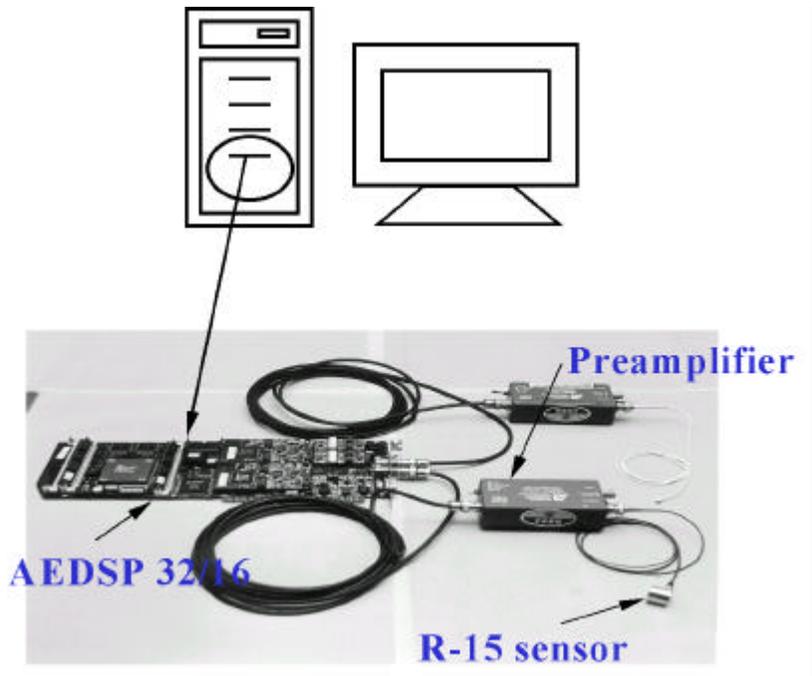


**Fig. 8** AEDSP 32/16 board and sensors.

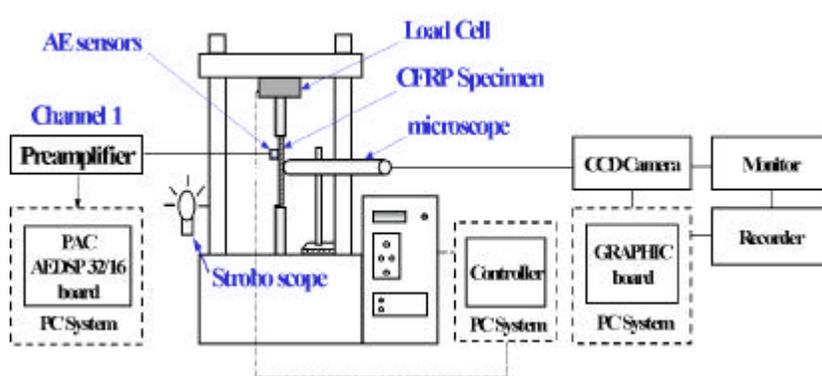
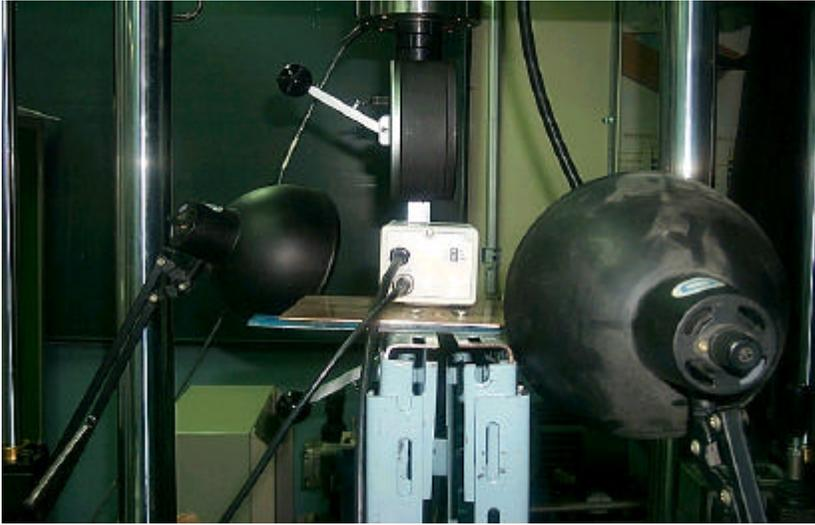


Fig. 9 Schematic diagram of experimental apparatus.



**Fig. 10** Photo of experimental apparatus.

## 4.

### 4.1

Fig. 11 (a), (b), (c) [0/90]s, [90/0]s [0/±45/90]s 3  
가 가 CFRP

- . 3  
- 가

가

가

Fig. 11 (a)

[0/90]s (b) [90/0]s 1424kg<sub>f</sub> 1420kg<sub>f</sub>

Fig. 11 (c) [0/±45/90]s

1002kg<sub>f</sub> 3가 가

, 1.5mm . [0/±

45/90]s Fig. 11 (a), (b) 227.6 229.8MPa

가 가 [0/±45/90]s

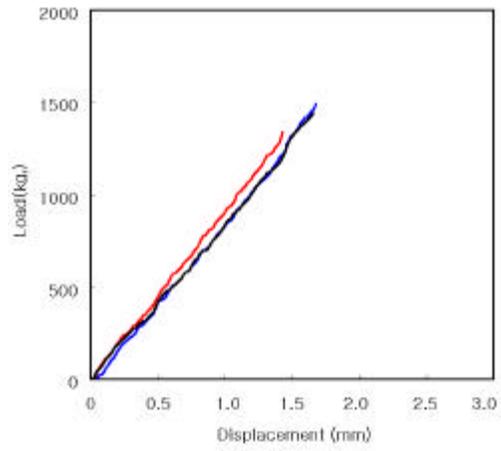
가 . ±45°

가 . Table 2

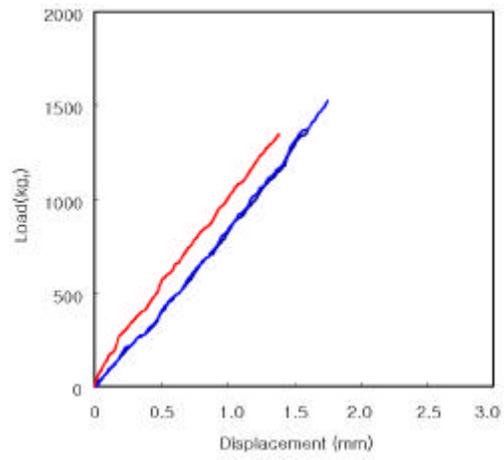
[0/±45/90]s 가

**Table 2** Variation of strength of tensile test results

	Ultimate tensile strength	Maximum Load	Modulus of elasticity	Fracture strain rate	poisson's ratio
Fiber orientation	$\sigma$ (MPa)	P (kgf)	E (GPa)	$\epsilon$ (%)	$\nu$
[0/90]s	775.6	1424	53.1	1.46	0.042
[90/0]s	773.4	1420	56.0	1.38	0.043
[0/ $\pm$ 45/90]s	545.8	1002	43.3	1.26	0.046
Average	698.3	1282	50.8	1.36	0.044

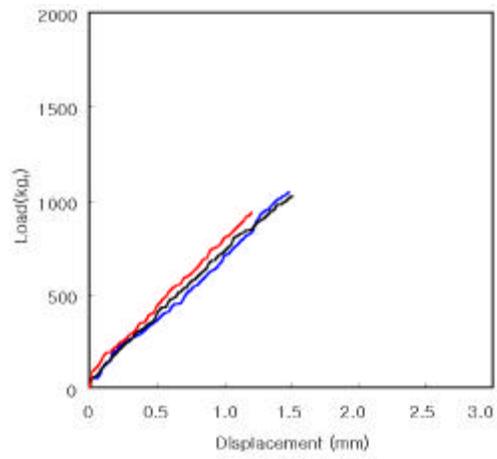


(a) [0/90]s



(b) [90/0]s

**Fig. 11** Load-displacement relationships.



(c) [0/ ± 45/90]s

**Fig. 11** Load-displacement relationships.

## 4.2 AE

Fig. 12 (a), (b), (c) [0/90]s, [90/0]s [0/±45/90]s 3가

CFRP AE 3

AE count

count (a) (c) , ,

, , ,

. Fig. 12 (a) [0/90]s

가 99

752kg<sub>f</sub> AE count가 2600 ,

가 count 가 가 153

13800 count

1163kg<sub>f</sub> . count가 18200 171.3

1341kg<sub>f</sub> . Fig. 12 (b) [90/0]s 18

75 833 count

가 count 가 가 171

13600 count가 29600

210.4 1527kg<sub>f</sub> . Fig. 12 (c) [0/±45/90]s

144.3 (a), (b)

938kg<sub>f</sub> . 가 39

69 489kg<sub>f</sub> 333

count 845kg<sub>f</sub> count

가 129 4033 가

가 count가 6867 144.3

[90/0]s, [0/90]s, [0/±

45/90]s count 가 . (a)

(b)

가

count가

Fig. 13

AE count

log-log

(2) (4)

가

P , AE<sub>c</sub> AE count

$$P = 86.085AE_c^{0.2712} \quad (2)$$

$$P = 49.127AE_c^{0.3346} \quad (3)$$

$$P = 164.13AE_c^{0.1925} \quad (4)$$

AE count 가 n 가 0.3346

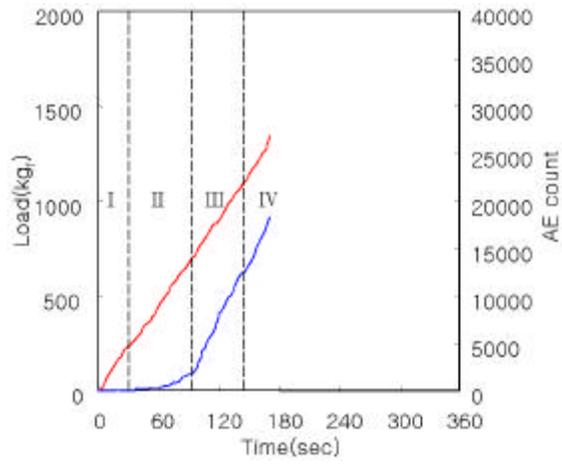
가 가 [0/90]s AE

count가 18200 n 0.2712

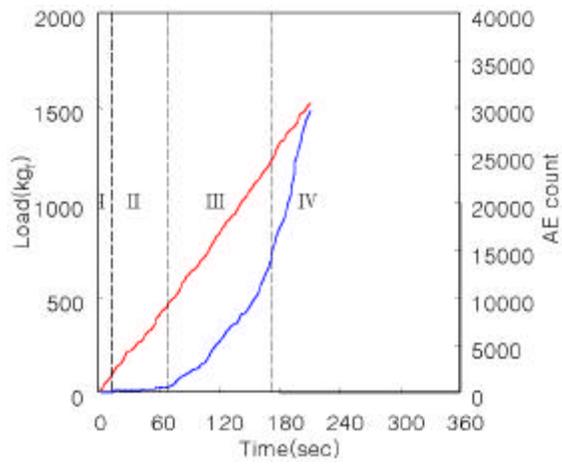
[0/±45/90]s가 가 n 0.1925

[90/0]s가 AE count 가 가

[0/90]s [0/±45/90]s

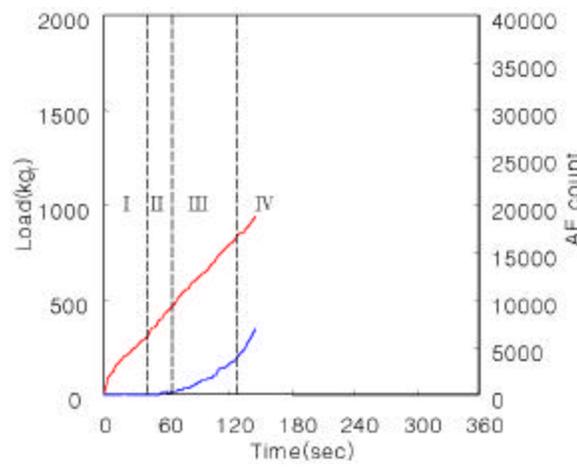


(a) [0/90]s



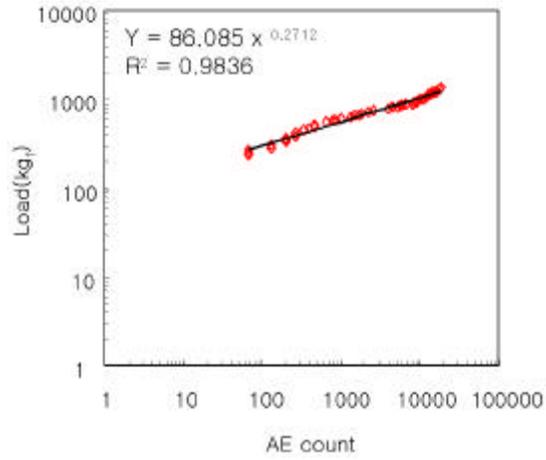
(b) [90/0]s

**Fig. 12** The relationships of load and AE count for tensile test time.

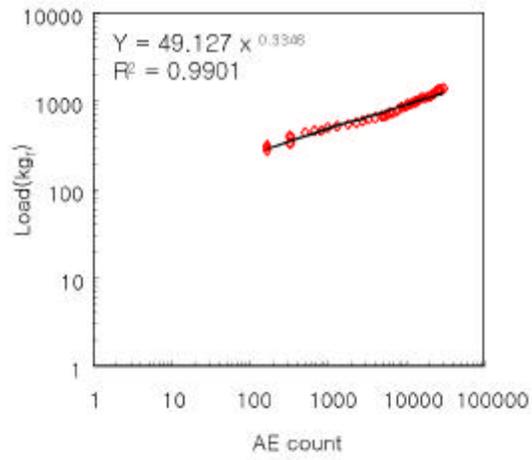


(c)  $[0^\circ \pm 45/90]_s$

**Fig. 12** The relationships of load and AE count for tensile test time.

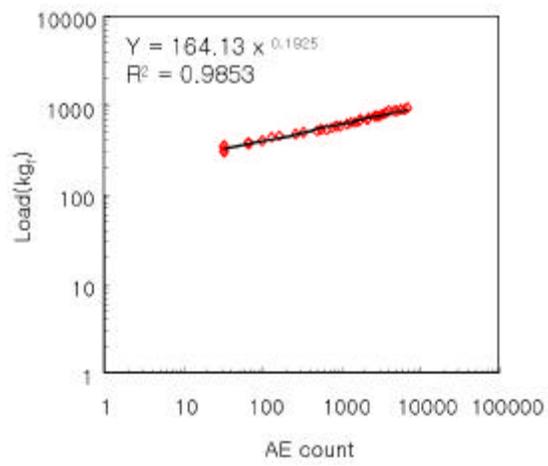


(a) [0/90]s



(b) [90/0]s

**Fig. 13** Load-AE count relationships.



(c)  $[0/\pm 45/90]_s$

**Fig. 13** Load-AE count relationships.

### 4.3

- [0/90]s [90/0]s  
 S-N Fig. 14 .  
 [0/90]s CFRP 95, 90,  
 85, 70% 30  $7.157 \times 10^6$   
 가 [90/0]s  
 95, 80%  
 가 . [0/90]s  
 가 ,  
 .  
 . [0/90]s [90/0]s

[90/0]s가 [0/90]s

Fig. 15 [90/0]s  
 80%  
 . (a/d) (a)  
 (d) . 가 0  $1 \times 10^5$   
 4.44  
 . 가  
 (Characteristic Damage State, CDS)<sup>(16)</sup>  
 $5 \times 10^5$  5.43  
 ,

가

.

가

$5 \times 10^5$

$1 \times 10^6$

8.46

.

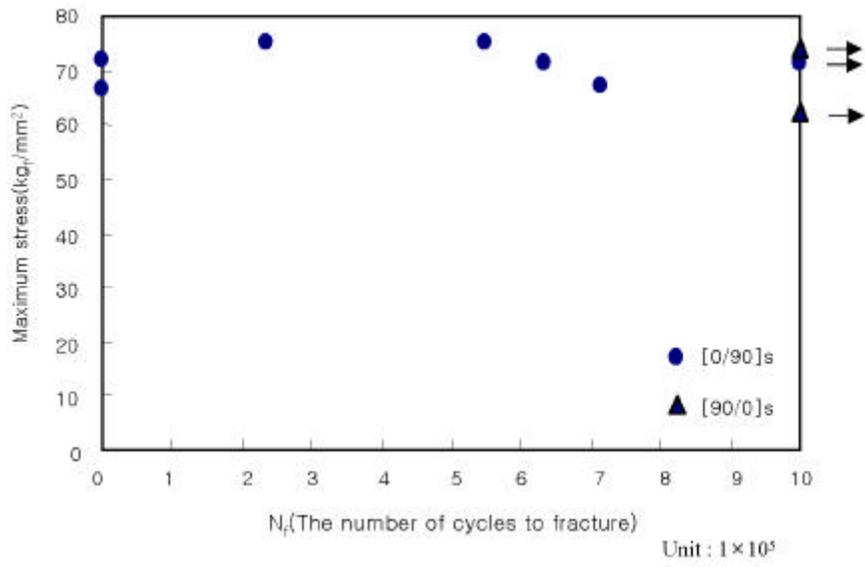


**Fig. 14** S-N Curve for CFRP specimen with hole(R=0.1).

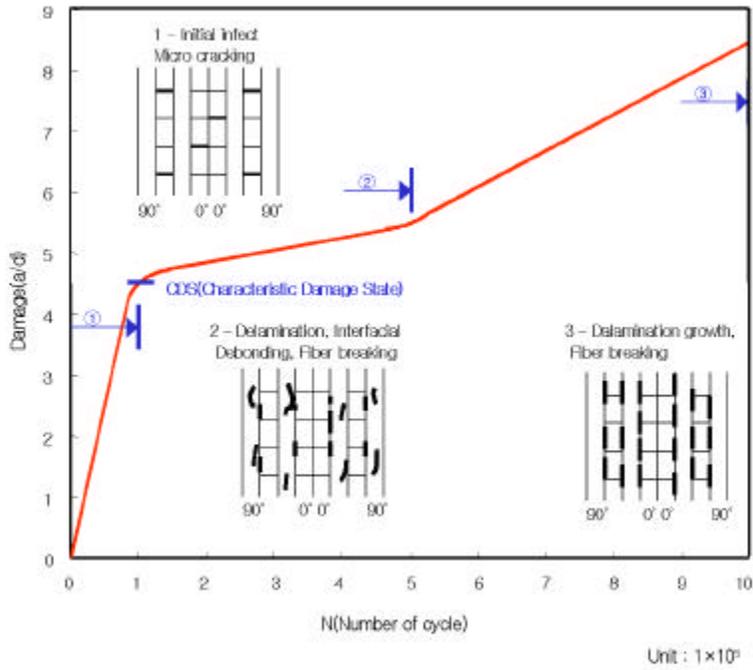


**Fig. 15** The development of damage during the fatigue life  
 ( $[90/0]_s$ ,  $\sigma_{max}/\sigma_u = 0.8$ ,  $R = 0.1$ ).

#### 4.4 CCD

Fig. 16 (a) (d) [0/ ± 45/ 90]s  
 S TR-850 CCD  
 . Fig. 16 (a)  
 . Fig. 16 (b) 296kg<sub>f</sub>  
 AE  
 count가 33.3 . Fig. 16 (c)  
 90%  
 855kg<sub>f</sub> . Fig. 16 (d) 938kg<sub>f</sub>  
 , AE count가  
 6867 . ± 4  
 5 ° ± 45 °  
 45 ° 가  
 45 ° ± 45 °  
 . Fig. 17 (a) (b) [0/ 90]s, [90/ 0]s  
 . [0/ ± 45/ 90]s  
 가 . Fig. 18 (a) (f) [90/ 0]s  
 80% 가  
 . (a)  
 . (b) 1 × 10<sup>5</sup>  
 . (c) 가 가

. (d) (e) 가 가  
 (f)  $1 \times 10^6$   
 .  
 2  $1 \times$   
 $10^6$   
 .  
 가 .

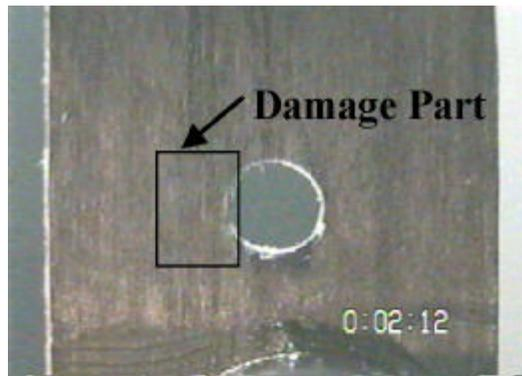


(a) Load=0kg<sub>r</sub>



(b) Load=296kg<sub>r</sub>

**Fig. 16** Photographs of video recording of fracture by tensile test ([0/ ± 45/90]s).



(c) Load=855kg<sub>r</sub>



(d) Load=938kg<sub>r</sub>

**Fig. 16** Photographs of video recording of fracture by tensile test ( $[0/\pm 45/90]_s$ ).



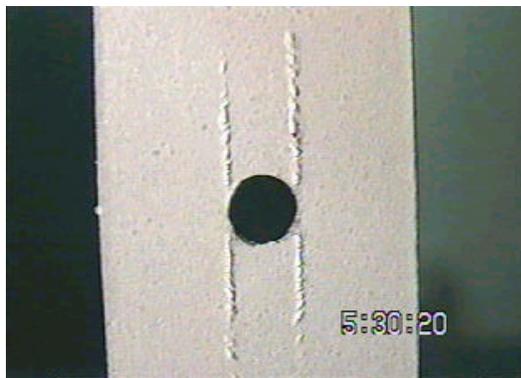
(a) [0/90]s

(b) [90/0]s

**Fig. 17** Photographs of fracture by tensile test.

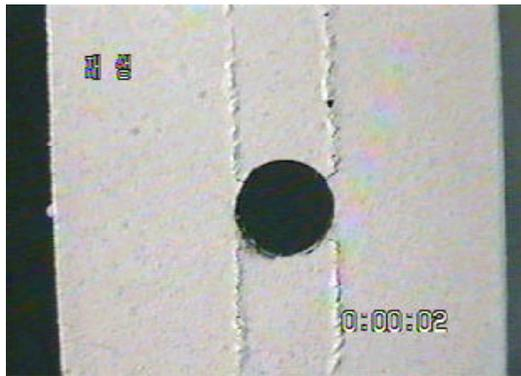


(a) 0cycle

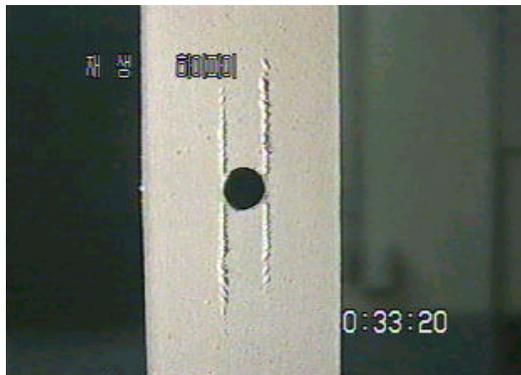


(b)  $1 \times 10^5$  cycle

**Fig. 18** Photographs of video recording of fracture by fatigue test (fatigue limit =  $1 \times 10^6$ ).

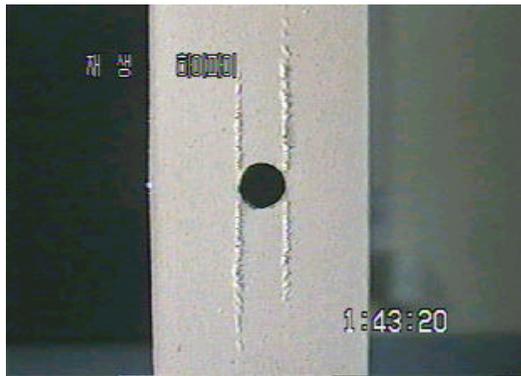


(c)  $3 \times 10^5$  cycle

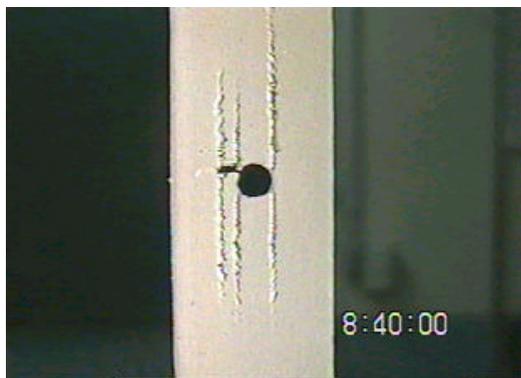


(d)  $5 \times 10^5$  cycle

**Fig. 18** Photographs of video recording of fracture by fatigue test (fatigue limit =  $1 \times 10^6$ ).



(e)  $7 \times 10^5$  cycle



(f)  $1 \times 10^6$  cycle

**Fig. 18** Photographs of video recording of fracture by fatigue test (fatigue limit =  $1 \times 10^6$ ).

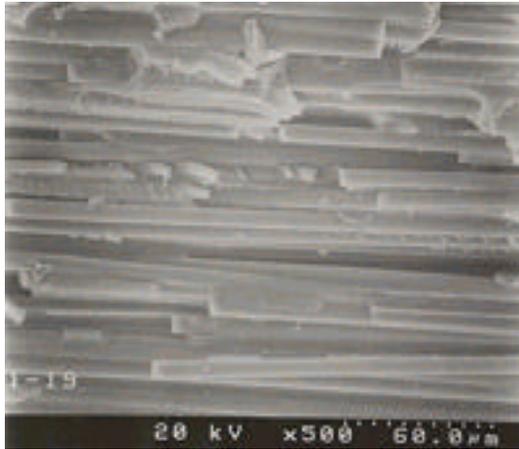
## 4.5 SEM

(SEM)  
Fig. 19 . Fig. 19 (a) [0/90]s  
가 . Fig. 19  
(b) (c) [90/0]s [0/±45/90]s  
. Fig. 19 (b) 90°  
0° 가  
. Fig. 19 (c) 45°  
Fig. 19 (d) 0°

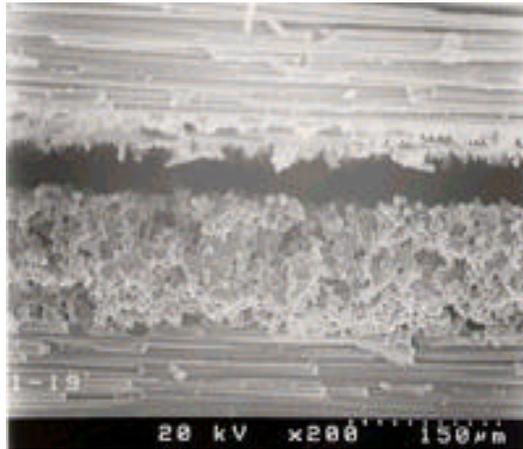
가 .  
SEM  
Fig. 20 . Fig. 20 (a)  
. 0° 90°  
가 가  
가 가  
가  
. Fig. 20 (b)  
,  
,  
. Fig. 20 (c)

. Fig. 20 (d)

.

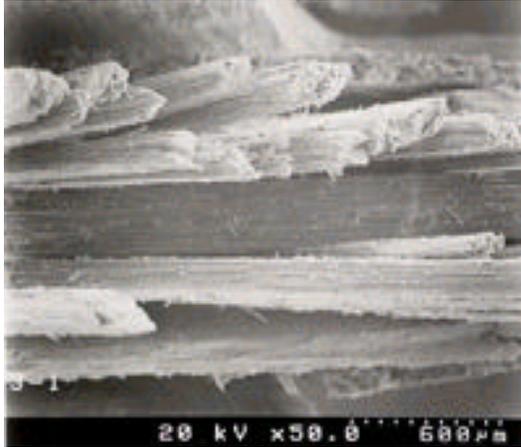


(a) [0/90]s

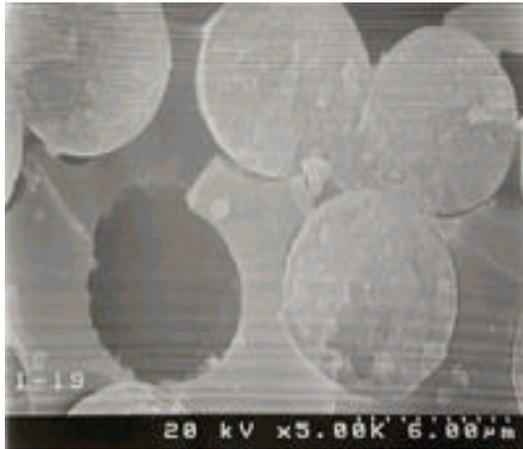


(b) [90/0]s

**Fig. 19** SEM photograph of side and fracture surface for after tensile test.

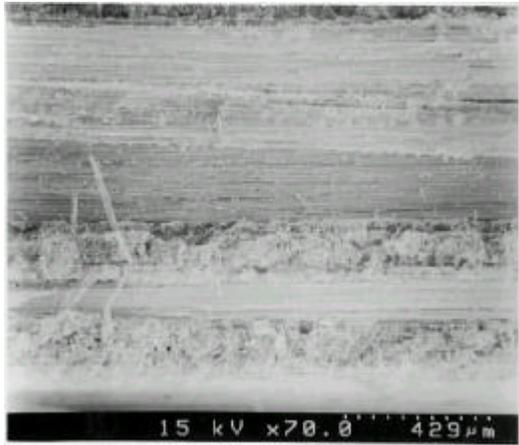


(c)  $[0/\pm 45/90]_s$

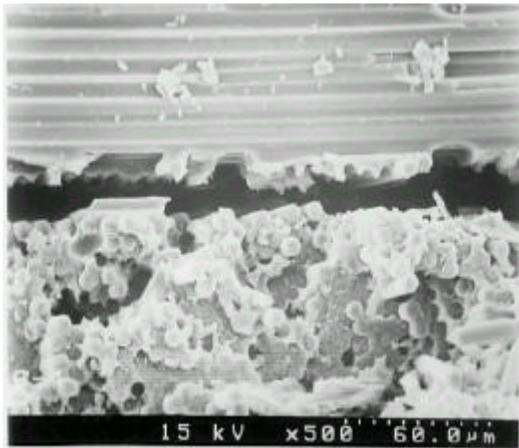


(d)  $[0/90]_s$

**Fig. 19** SEM photograph of side and fracture surface for after tensile test.

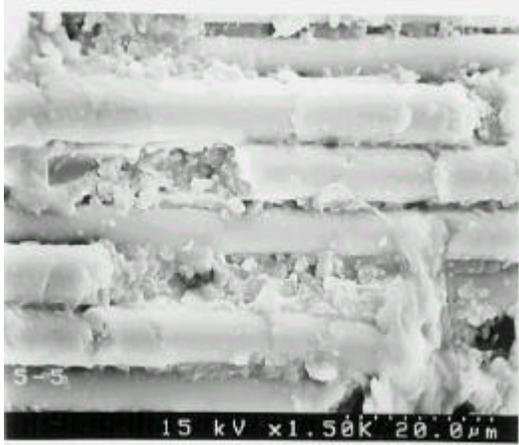


(a) [90/0]s

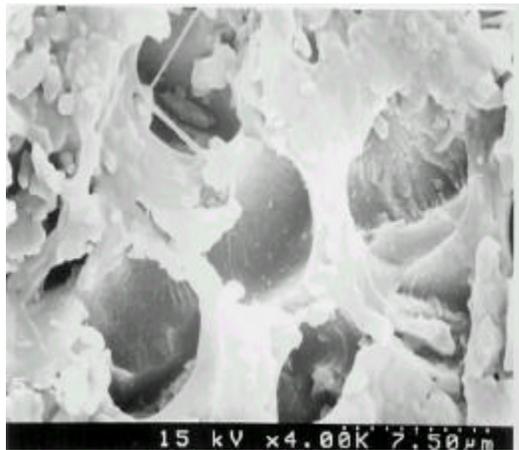


(b) [90/0]s

**Fig. 20** SEM Photograph of side and fracture surface for after fatigue test.



(c) [0/90]s



(d) [0/90]s

**Fig. 20** SEM Photograph of side and fracture surface for after fatigue test.

## 5.

가 [0/90]s, [90/0]s  
 [0/ ±45/90]s CFRP  
 AE 가 ,  
 CCD SEM  
 가

1. [0/90]s [90/0]s  
 가 [0/ ±45/90]s  
 ±45 °

2. AE count , ,  
 , I, , ,  
 , AE count [90/0]s 가 29600 가  
 [0/90]s 18200, [0/ ±45/90]s가 6867 가  
 AE count 가 .

3. [90/0]s 80%  
 , 0 1×  
 10<sup>5</sup> 4.44 5×  
 10<sup>5</sup>  
 가 1×10<sup>6</sup> 8.46

4. CCD

[0/ ±

45/90]s

45 °

가

5.

[90/0]s

80%

가

$1 \times 10^6$

가

6. SEM

가

- (1) , " ", , 30 ,  
2 , pp. 172 179, 1990.
- (2) Ogin, S. L. Smith, P. A. and Beaumont, P. W. R., "Matrix cracking and stiffness reduction during the fatigue of  $[0/90_2]_s$  GFRP laminate", Composite Science and Technology, Vol. 22, pp. 22 31, 1985.
- (3) Tsai, C. L. and Daniel, I. M., "The behavior of cracked cross-ply composite laminates under general in-plane loading", Damage in Composite Materials, ed. G. Z. Voyiadjis, Elsevier, pp. 51 66, 1993.
- (4) Boller, K. H., Modern Plastics, 41, No. 10, pp. 146, 1964.
- (5) Owen, M. J. and Bishop, P. T., "Crack-growth relationship for glass-reinforced Plastics and their application to design", J. phys., Vol. 7, pp. 1214, 1974.
- (6) Lawcock, G. L. Ye and Mai, Y., "Progressive Damage and Residual Strength of a Carbon Fiber Reinforced Metal Laminate", Journal of Composite Materials, Vol. 31, No. 8, pp. 762 787, 1997.
- (7) , I. M. Daniel, "  
AE , 11 , 5 , pp.  
14 21, 1998.
- (8) Ni, Q. Q. and Jinen, E., "Fracture Mechanism and Acoustic Emission of short Carbon Fiber Reinforced Nylon", Society.

- Mater. Science.(Japan), Vol. 42, pp. 255, 1993.
- (9) Ni, Q. Q. and Jinen, E., "Fracture Behavior and Acoustic Emission of SFC", Society. Mater. science.(Japan), Vol. 42, pp. 561, 1993.
- (10) Ni, Q, "Fracture Behavior and Acoustic Emission in Bending Test on single-fiber Composites", Engineering. Fracture Mechanics, Vol. 56, pp. 779, 1997.
- (11) Chow, T. M. Hutchins, D. A. and Mottram, J. T., "Simultaneous acoustic emission and ultrasonic tomography imaging in anisotropic polymer composite-material", Journal of Acoustical Society of America, Vol. 94, pp. 944 953, 1993.
- (12) J. S. Huh., "Fatigue Life Prediction of Circular Notched Composite Laminnates", , 1994.
- (13) Agarwal and J. W. Dally, B. D., "Prediction of Low-Cycle Fatigue Behavior of GFRP", An Expermental Approach, J. Mater, Science, pp. 193 199, 1975.
- (14) , " ", , 34 , 1 , pp. 20 32, 1994.
- (15) Standard test method for "tensile properties of polymer matrix composite materials", ASTM D3039, 2000.
- (16) Reifsnider, K. L., Proceedings. 14th Annual Society of Engineering science Meeting, Lehigh University, Bethlehem, pp. 14 16, 1977.

**Evaluation of the Mechanical Properties and Fatigue Damage  
on Lay-up Orientation of Carbon Fiber Reinforced  
Plastic Composite**

Young-Il Tae

*Department of Safety Engineering, Graduate school,  
Pukyong National University*

**Abstract**

In recent years, advanced composites like CFRP are increasingly used in various industry fields because of their unique specific strength and stiffness properties. However CFRP laminate composites bring on the problems as like the delamination, matrix cracking, debonding, fiber breaking. These complex damage mechanism depend on the material, lay-up sequence, geometry and loading condition.

The purpose of study is the estimation of the fatigue damage mechanism and mechanical properties effected by lay-up orientation for CFRP laminate composite with the hole notch. The tensile tests for  $[0/90]_s$ ,  $[90/0]_s$ , and  $[0/\pm 45/90]_s$  laminate composite were accomplished with acoustic sensor and failure processes were recorded by CCD video camera in real time. The analysis of cumulate AE count was done by AE analysis software (MISTRAS-2001). Also SEM examination for fracture and side surface were carried out. In addition, fatigue tests were carried out for CFRP of  $[0/90]_s$ ,  $[90/0]_s$  lay-up recording damage processes of surface by CCD video camera in each cycle.

From this study, the following conclusions could be drawn.

1. Mechanical properties were obtained and they were similar between two kinds of cross-ply orientation in CFRP laminate composites, however cumulate AE count,

regardless of lay-up orientation, was increased on tensile test according to increasing the load,

2. The damage length according to the fatigue repeat cycles was expressed as three stages in [90/0]<sub>s</sub> laminate composite.

3. Fatigue damage failure mechanism of [0/90]<sub>s</sub>, [90/0]<sub>s</sub> laminate composite involves splitting, fiber-matrix debonding as well as delamination and fiber breaking which promotes the fracture.

These results will be useful for development of the newer composite properties and failure prevention of composite structures.

가

,  
가

.

,

,

,

,

,

,

.

.

,

,

,

,

,

,

,

.

,

,

,

,

.

,

,

,

.

2002 2